

tion of the protein in the cell would have the same functional result as SV40 large T antigen, adenovirus E1B 55-kD protein, or a mutated form of the p53 protein in eliminating wild-type p53 and thus preventing it from its function as a regulator of cell growth.

REFERENCES AND NOTES

- H. Zur Hausen and A. Schneider, in *The Papillomaviruses*, vol. 2 of *The Papovaviridae*, P. M. Howley and N. P. Salzman, Eds. (Plenum, New York, 1987), pp. 245–263.
- R. Schlegel, W. C. Phelps, Y.-L. Zhang, M. Barbosa, *EMBO J.* **7**, 3181 (1988); A. Storey *et al.*, *ibid.*, p. 1815; C. D. Woodworth, J. Doninger, J. A. DiPaolo, *J. Virol.* **63**, 159 (1989).
- C. C. Baker *et al.*, *J. Virol.* **61**, 962 (1987); H. Shirasawa *et al.*, *ibid.* **62**, 1022 (1988).
- E. Schwarz *et al.*, *Nature* **314**, 111 (1985); A. Schneider-Gadicke and E. Schwarz, *EMBO J.* **5**, 2285 (1986); D. Smotkin and F. O. Wettstein, *Proc. Natl. Acad. Sci. U.S.A.* **83**, 4680 (1986).
- K. Münger, W. C. Phelps, V. Bubb, P. M. Howley, R. Schlegel, *J. Virol.* **63**, 4417 (1989); P. Hawley-Nelson, K. H. Vousden, N. L. Hubbard, D. R. Lowy, J. T. Schiller, *EMBO J.* **8**, 3905 (1989).
- J. A. DeCaprio *et al.*, *Cell* **54**, 275 (1988).
- P. Whyte *et al.*, *Nature* **334**, 124 (1988).
- N. Dyson, P. M. Howley, K. Münger, E. Harlow, *Science* **243**, 934 (1989).
- K. Münger, B. A. Werness, N. Dyson, E. Harlow, P. M. Howley, *EMBO J.* **8**, 4099 (1989).
- S. Watanabe, T. Kanda, K. Yoshiike, *J. Virol.* **63**, 965 (1989).
- D. P. Lane and L. V. Crawford, *Nature* **278**, 261 (1979).
- D. I. H. Linzer and A. J. Levine, *Cell* **17**, 43 (1979).
- P. Sarnow, Y. S. Ho, J. Williams, A. J. Levine, *Cell* **28**, 387 (1982).
- J. R. Jenkins, K. Rudge, G. A. Curries, *Nature* **312**, 651 (1984).
- D. Elyahu, A. Raz, P. Gruss, D. Givol, M. Oren, *ibid.*, p. 646; L. F. Parada, H. Land, R. A. Weinberg, D. Wolf, V. Rotter, *ibid.*, p. 649.
- B. Rovinski and S. Benchimol, *Oncogene* **2**, 445 (1988).
- C. A. Finlay *et al.*, *Mol. Cell. Biol.* **8**, 531 (1988).
- D. Elyahu *et al.*, *Oncogene* **3**, 313 (1988).
- P. Hinds, C. Finlay, A. J. Levine, *J. Virol.* **63**, 739 (1989).
- C. A. Finlay, P. W. Hinds, A. J. Levine, *Cell* **57**, 1083 (1989).
- H. Masuda, C. Miller, H. P. Koeffler, H. Battifora, M. J. Cline, *Proc. Natl. Acad. Sci. U.S.A.* **84**, 7716 (1987).
- B. Vogelstein *et al.*, *Science* **244**, 207 (1989); S. J. Baker *et al.*, *ibid.*, p. 217.
- D. Pennica *et al.*, *Virology* **134**, 477 (1984).
- E. Harlow, L. V. Crawford, D. C. Pim, N. M. Williamson, *J. Virol.* **39**, 861 (1981).
- J. W. Yewdell, J. V. Gannon, D. P. Lane, *ibid.* **59**, 444 (1986).
- B. A. Werness and P. M. Howley, unpublished results.
- J. T. Schiller, W. C. Vass, D. R. Lowy, *Proc. Natl. Acad. Sci. U.S.A.* **81**, 7880 (1984); Y. C. Yang, H. Okayama, P. M. Howley, *ibid.* **82**, 1030 (1985).
- R. Zakut-Houri, B. Bienz-Tadmor, D. Givol, M. Oren, *EMBO J.* **4**, 1251 (1985).
- J. Field *et al.*, *Mol. Cell. Biol.* **8**, 2159 (1988).
- N. C. Reich and A. J. Levine, *Nature* **308**, 199 (1984); J. A. DeCaprio *et al.*, *Cell* **58**, 1085 (1989); P.-L. Chen, P. Scully, J.-Y. Shew, J. Y. Wang, W.-H. Lee, *ibid.*, p. 1193.
- M. Mowat, A. Cheng, N. Kimura, A. Bernstein, S. Benchimol, *Nature* **314**, 633 (1985).
- T. Takahashi *et al.*, *Science* **246**, 491 (1989).
- N. C. Reich, M. Oren, A. J. Levine, *Mol. Cell. Biol.* **3**, 2143 (1983).
- G. Matlashewski, L. Banks, D. Pim, L. Crawford, *Eur. J. Biochem.* **154**, 665 (1986).
- W. C. Phelps, C. L. Yec, K. Münger, P. M. Howley, *Cell* **53**, 539 (1988).
- U. K. Laemmli, *Nature* **227**, 680 (1970).
- W. M. Bonner and R. A. Laskey, *Eur. J. Biochem.* **46**, 83 (1974).
- Sequences of the oligonucleotide primers used for PCR amplification were: HPV-6b 5' sense, CAGTC-GACACCATGGAAGTGC AAATGCTCC and 3' antisense, GTAAGCTTTAGGGTAACATGTCT-TCC; HPV-11 5' sense, GCGTCGACCACCATGG-AAAGTAAAGATG and 3' antisense, GCAAGCTT-AGGGTAAACAAGTCTTC; HPV-18 5' sense, GCGTCGACCACCATGGCGCGCTTTGAG and 3' antisense, GCAAGCTTACTTGTGTTTCTC; BPV-1 5' sense, GCGTCGACCACCATGGACCT-GAAACCTTTTG and 3' antisense, GCAAGCTTCTATGGGTATTTGGACCTTG.
- The 3' antisense primers for HPV-11 and HPV-18 were the same as those used to clone the wild-type E6 ORFs. For HPV-16, the E7 3' antisense oligonucleotide primer 5'-GGTACCTGCAGGATCAGCCATG-3' was used. The 5' oligonucleotide primer sequences used were (5'-3'): HPV-11 E6, GCGTCGACCACCATGTACCCGTACGACGTGCCGGACTACGCGAGCCTGCCGGCCTGGAAAGTAAAGATGCTCCAC; HPV-16 E6, GCGTCGACCACCATGTACCCGTACGACGTGCCGGACTACGCGAGCCTGCCGGCCTGTTTCAGGACCCACAGGAGCG; HPV-18 E6, GCGTCGACCACCATGTACCCGTACGACGTGCCGGACTACGCGAGCCTGCCGGCCTGGCGCGCTTTGAGGATCCAAC.
- F. I. Schmeig and D. T. Simmons, *Virology* **164**, 132 (1988).
- We are grateful to J. Bolen, K. Münger, and R. Schlegel for a critical reading of the manuscript. We thank J. Bolen, N. Dyson, E. Harlow, and K. Münger for helpful discussions during the course of this study, and J. Byrne for oligonucleotide synthesis. B.A.W. was supported by a National Research Council-NIH Research Associateship.

11 December 1989; accepted 15 February 1990

EGF Receptor and *erbB-2* Tyrosine Kinase Domains Confer Cell Specificity for Mitogenic Signaling

PIER PAOLO DI FIORE,* ORESTE SEGATTO, WILLIAM G. TAYLOR, STUART A. AARONSON, JACALYN H. PIERCE

The epidermal growth factor (EGF) receptor (EGFR) can efficiently couple with mitogenic signaling pathways when it is transfected into interleukin-3 (IL-3)-dependent 32D hematopoietic cells. When expression vectors for *erbB-2*, which is structurally related to EGFR, or its truncated counterpart, Δ *NerbB-2*, were introduced into 32D cells, neither was capable of inducing proliferation. This was despite overexpression and constitutive tyrosine kinase activity of their products at levels associated with potent transformation of fibroblast target cells. Thus, EGFR and *erbB-2* couple with distinct mitogenic signaling pathways. The region responsible for the specificity of intracellular signal transduction was localized to a 270-amino acid stretch encompassing their respective tyrosine kinase domains. Thus, tissue- or cell-specific regulation of growth factor receptor signaling can occur at a point after the initial interaction of growth factor with receptor. Such specificity in signal transduction may account for the selection of certain oncogenes in some malignancies.

THE INTERACTION OF GROWTH FACTORS with specific membrane receptors triggers a series of intracellular events that are of critical importance in the regulation of normal cell proliferation. Subversion of these mitogen-responsive pathways plays a determinant role in the neoplastic process (1). Little is known about the nature of such signaling pathways and the specificity of receptor-pathway coupling. The cDNA of a foreign receptor introduced into a naïve cell can confer responsiveness to its ligand, indicating that regulation of cell proliferation involves growth factor receptor expression and ligand availability (2, 3). Intracellular specificity in signaling pathways may also exist as indicated by findings that different subsets of cellular proteins are

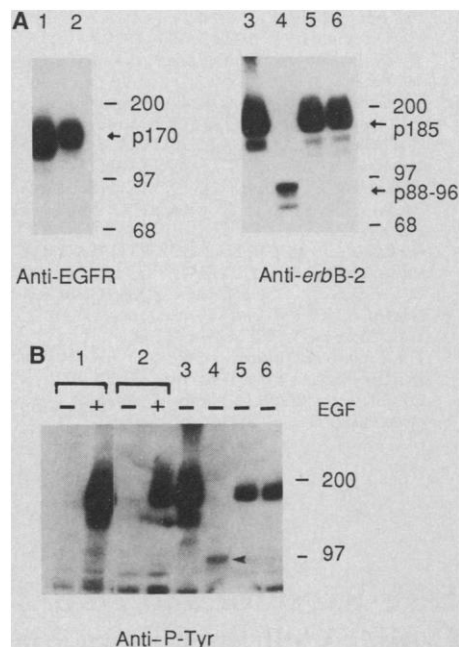
phosphorylated in response to various growth factors (4).

EGFR and *erbB-2* genes differ in their efficiency of transformation for NIH 3T3 fibroblasts, suggesting that they may couple with different efficiency to one or more intracellular signal transduction pathways (5, 6). We initially sought to compare mitogenic signaling by these two genes in the hematopoietic line 32D, which lacks either receptor and is normally dependent on interleukin-3 (IL-3) for proliferation (7). For this purpose the eukaryotic expression vectors, LTR-EGFR (6) and LTR-*erbB-2* (5), were transfected into 32D cells by electroporation (8). These vectors contained the transcriptional initiation sequences of the Moloney murine leukemia virus (M-MuLV) long terminal repeat, along with the *Ecogpt* selectable marker (9), which confers resistance to mycophenolic acid (9). After transfection and marker selection, viable cell lines designated 32D-EGFR and 32D-*erbB-2*

Laboratory of Cellular and Molecular Biology, National Cancer Institute, National Institutes of Health, Bethesda, MD 20892.

*To whom correspondence should be addressed.

Fig. 1. Comparison of protein and tyrosine phosphorylation levels of EGFR and *erbB-2* expressed in NIH 3T3 (lanes 1 and 3) or 32D (lanes 2 and 4 to 6) transfectants. NIH 3T3 and 32D cells were transfected with the LTR-EGFR (lanes 1 and 2), LTR-*erbB-2* (lanes 3 and 5), LTR- Δ N*erbB-2* (lanes 4), and LTR-*erbB-2*Glu (lanes 6) expression vectors by electroporation (8) or by the calcium phosphate precipitation method (5), respectively, as described (2, 5). Cells were then selected by their ability to grow in medium supplemented with mycophenolic acid (9) and stable transfected cell lines were established. (A) Total cell lysates (50 μ g) from NIH 3T3 or 32D cell lines were fractionated by SDS-polyacrylamide gel electrophoresis (SDS-PAGE) and transferred to nitrocellulose filters. Detection was performed with either the E7 (anti-EGFR) (28) or the M6 (anti-*erbB-2*) (28) anti-peptide antibodies coupled to 125 I-labeled protein A, as described (5). (B) Total cell lysates (50 μ g) from NIH 3T3 or 32D cell lines were fractionated by SDS-PAGE and transferred to nitrocellulose. Detection of phosphotyrosine-containing proteins was performed with an affinity-purified antibody to phosphotyrosine (anti-P-Tyr) coupled to 125 I-labeled protein A (5). Specificity of immunodetection for the E7 and M6 antibodies was controlled by performing parallel staining of identical blots with antibodies absorbed with the specific peptides (2 mg/ml). In the case of the anti-P-Tyr, specificity was controlled by preabsorption of the antibody with either phosphotyrosine, phosphoserine, or phosphothreonine. Recognition of EGFR and *erbB-2* proteins was completely abolished by preabsorption of the anti-P-Tyr with phosphotyrosine, although it was not affected by competition with phosphoserine or phosphothreonine (not shown). Sizes are shown in kilodaltons. The arrows point at the EGFR (p170), *erbB-2* (p185), and Δ N*erbB-2* (p88-96) proteins.



were established. Immunoblot analysis revealed that these transfectants synthesized high levels of gp170-EGFR and gp185^{*erbB-2*}, respectively (Fig. 1A). The two products synthesized in 32D cells were indistinguishable in size from EGFR or gp185^{*erbB-2*} proteins overexpressed in transfected NIH 3T3 fibroblasts (Fig. 1A) or in human tumor cell lines (5, 6, 10, 11). Moreover, the levels of gp185^{*erbB-2*} or EGFR detected in 32D cells were comparable to those associated with induction of the malignant phenotype in NIH 3T3 cells (Fig. 1A) (5, 6).

The ability of the receptors to become phosphorylated on tyrosine in vivo has been found to correlate well with the level of receptor activation (12, 13). Tyrosine phosphorylation of EGFR in 32D-EGFR cells was only observed in the presence of EGF (Fig. 1B). In contrast, gp185^{*erbB-2*} expressed by 32D-*erbB-2* transfectants showed significant levels of endogenous tyrosine phosphorylation. Similar levels of EGFR and gp185^{*erbB-2*} tyrosine phosphorylation were observed in transfected NIH 3T3 cells (Fig. 1B).

To compare the biological effects of gp185^{*erbB-2*} and EGFR expression in 32D cells, we analyzed the growth characteristics of the transfectants by colony formation in semisolid medium. This is a stringent test of mitogenic signaling capacity since several cycles of cell division are required to form a detectable colony. In each case, colony formation was standardized relative to colony forming ability in the presence of serum plus IL-3. 32D-EGFR cells did not form colonies in soft agar in the absence of EGF but responded dramatically to EGF addition (Fig. 2). In contrast, the growth properties of 32D-*erbB-2* cells were indistinguishable from those of control 32D, in that they could not proliferate in serum alone or supplemented with EGF but promptly responded to IL-3 (Fig. 2). In NIH 3T3 cells *erbB-2* was 100 times as potent as EGFR as a transforming gene (5, 6) (Fig. 2). Since gp185^{*erbB-2*} was expressed at high levels in 32D-*erbB-2* cells and exhibited constitutive tyrosine phosphorylation, these results strongly suggested that gp185^{*erbB-2*} was inefficient relative to EGFR at coupling with intracellular mitogenic signaling pathways in 32D cells.

To further test this hypothesis, we transfected 32D cells with the LTR- Δ N*erbB-2* and LTR-*erbB-2*Glu expression vectors, which encode an NH₂-truncated *erbB-2* protein lacking the majority of its extracellular domain (5) and an *erbB-2* protein bearing a single Val to Glu mutation in the transmembrane region (12), respectively. These two mutant *erbB-2* proteins have enhanced transforming potential in NIH 3T3 cells and higher intrinsic tyrosine kinase activity relative to the wild type (5, 12) (Fig. 2). Enzymatically active

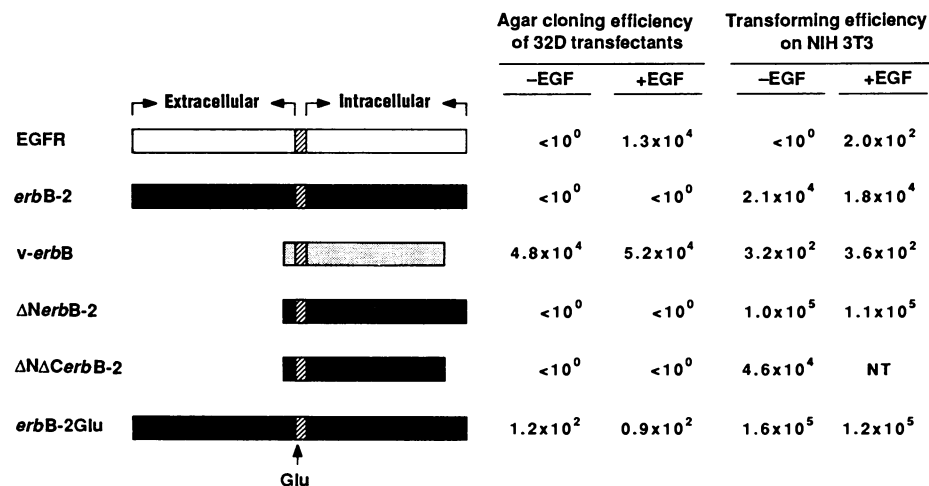
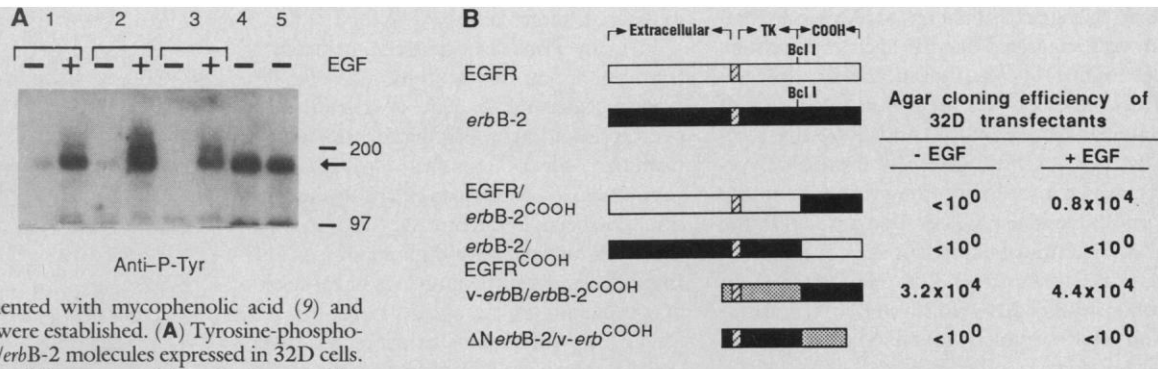


Fig. 2. Comparison of biological activity of EGFR and *erbB-2* expressed in 32D and NIH 3T3 cells. The indicated expression vectors, engineered as described (5, 6, 14, 15), were transfected in 32D cells by electroporation (8) or in NIH 3T3 cells by the calcium phosphate precipitation method (5). Cloning efficiency of 32D transfectants: 32D transfectants, after selection in a medium containing mycophenolic acid (9), were tested for their requirement for growth factors by assaying their capability to form colonies in semisolid medium supplemented with the indicated growth factors. The cloning efficiency was established by plating cells at various concentrations in Iscove's modified Dulbecco's medium supplemented with 15% fetal bovine serum (Gibco) and 0.48% sea plaque agarose (Marine Colloids). EGF (100 ng/ml, Collaborative Research) was included when specified. Plates were incubated at 37°C in 5% CO₂. Visible colonies were scored at 12 days after plating. Values are presented as a fraction of the number of colonies that developed in medium supplemented with serum and IL-3 at 50 U/ml (Genzyme) (colonies/IL-3 colonies \times 10⁵). In each case the efficiency of growth in agar in the presence of IL-3 was around 30%. Values shown represent the average of three independent experiments, performed in duplicate. In each case standard error was less than 10% of the mean. Transforming efficiency on NIH 3T3: Transfection was performed with 40 μ g of calf thymus DNA as a carrier. Focus formation on NIH 3T3 cells was scored after 21 days on duplicate plates. Where indicated, EGF (20 ng/ml) was added at day 14 and cells were cultivated in the presence of the growth factor until day 21. The transformation efficiency was calculated in focus-forming units per picomole of cloned DNA added, based on the relative molecular weights of the respective plasmids. White bars, EGFR sequences; black bars, *erbB-2* sequences; dotted bars, *v-erbB* sequences; and Glu, glutamic mutation in the transmembrane (hatched) region of *erbB-2*Glu.

Fig. 3. Expression and biological activity of COOH chimeric molecules between EGFR and *erbB-2* expressed in 32D cells. The expression vectors, engineered as described (19, 20), were transfected in 32D cells by electroporation (8). Cells were then selected by their ability to grow in medium supplemented with mycophenolic acid (9) and stable transfected cell lines were established. (A) Tyrosine-phosphorylation of chimeric EGFR/*erbB-2* molecules expressed in 32D cells. Total cell lysates from 32D cell lines were subjected to immunoblot analysis, and immunodetection was performed with the panel of antibodies to various peptides (M1, M6, M7, E5, E7, and α F) described in (28). After densitometric analysis of the blots, the relative levels of the expressed proteins were calculated on the basis of the fact that each antibody recognized a parental and a chimeric molecule. Then equal amounts of receptor proteins [lanes 1 and 2, EGFR/*erbB-2*^{COOH} (numbers 1 and 2 represent independent electroporations); lane 3, EGFR; lane 4, *erbB-2*/EGFR^{COOH}; lane 5, *erbB-2*] were fractionated by SDS-PAGE, transferred to nitrocellulose, and immunodetected with the affinity-purified antibody to



phosphotyrosine (anti-P-Tyr). Specificity of the immunodetection was controlled as indicated in the legend to Fig. 1B. Sizes are shown in kilodaltons. (B) Biological activity of chimeric EGFR/*erbB-2* molecules expressed in 32D cells. The cloning efficiency was established as indicated in the legend to Fig. 2. Values shown represent the average of three independent experiments performed in duplicate. In each case standard error was less than 10% of the mean. White bars, EGFR sequences; black bars, *erbB-2* sequences; dotted bars, v-*erbB* sequences; and hatched bars, transmembrane region.

p88-96 Δ NerbB-2 and gp185^{erbB-2}Glu were readily detected in the transfected cells, as indicated by their high phosphotyrosine content (Fig. 1). The 32D- Δ NerbB-2 cells did not proliferate in soft agar in the absence of IL-3 (Fig. 2). 32D-*erbB-2*Glu formed some colonies in soft agar, but at approximately 1/100 the frequency exhibited by 32D-EGFR cultivated in the presence of EGF. Another expression vector, LTR- Δ N Δ CerbB-2 (14), engineered to express an *erbB-2* protein with NH₂- and COOH-terminal truncations, was unable to relieve 32D cells of their IL-3 dependence. In contrast, v-*erbB*, the activated counterpart of EGFR (which also has NH₂- and COOH-terminal truncations) (15, 16), abrogated IL-3 requirements (Fig. 2).

There was a very good correlation between agar growth and ability to incorporate [³H]thymidine during a 24-hour labeling period. Under conditions in which 32D transfectants failed to form colonies, there was little, if any, thymidine incorporation. The 32D-*erbB-2*Glu cells, which were very inefficient at colony formation (Fig. 2), exhibited 5 to 10% of the [³H]thymidine incorporation observed in the presence of IL-3 (17).

On the basis of the overall structural and sequence similarity of EGFR and *erbB-2*, we reasoned that chimeric molecules engineered by switching similar domains might retain functional integrity but acquire different signaling specificity. A comparison of the published sequences of EGFR and *erbB-2* cDNAs (18) revealed that their intracellular portions can be subdivided into two domains. The first, adjacent to the transmembrane sequence, encompasses the tyrosine kinase region and shows ~80% homology over a 275-amino acid stretch. This similarity drops dramatically over the ~300 amino acids of the COOH-

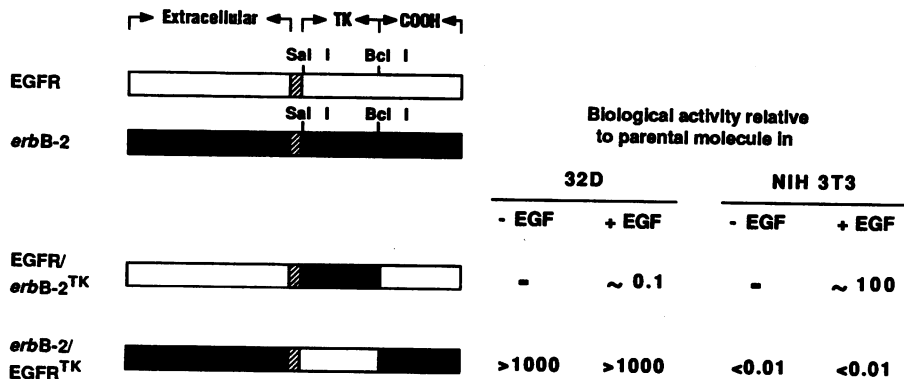


Fig. 4. Biological activity of tyrosine kinase chimeric molecules between EGFR and *erbB-2*, expressed in 32D and NIH 3T3 cells. The indicated expression vectors, engineered as described (21), were transfected in 32D cells by electroporation (8) or in NIH 3T3 cells by the calcium phosphate method (5). 32D transfectants, after selection in a medium containing mycophenolic acid (9), were tested for their capability to form colonies in semisolid medium supplemented with EGF, as described in the legend to Fig. 2. The transfection assay on NIH 3T3 cells was performed and the transforming efficiency was calculated as indicated in the legend to Fig. 2. Values are presented as biological activity of the chimeric molecules relative to the parental molecules (EGFR/*erbB-2*^{TK} versus EGFR and *erbB-2*/EGFR^{TK} versus *erbB-2*, respectively), whose biological activities in 32D and NIH 3T3 cells were assumed as 1. The results shown are typical and representative of three independent experiments performed in duplicate. White bars, EGFR sequences; black bars, *erbB-2* sequences; and hatched bars, transmembrane region.

terminal domain. To test whether the specificity for mitogenic signal transduction might segregate with their highly divergent COOH-terminal domains, we engineered chimeric expression vectors using a conserved Bcl I site located at the border between the two domains in EGFR and *erbB-2* cDNAs (19) (Fig. 3B). The LTR-EGFR/*erbB-2*^{COOH} expression vector encoded an EGFR-like molecule in which the last 263 amino acids of the EGFR molecule were replaced by the 300 amino acids of the analogous COOH-terminal domain of the *erbB-2* protein (19). The LTR-*erbB-2*/EGFR^{COOH} expression vector encoded the reciprocal chimeric protein (19).

The *erbB-2*/EGFR^{COOH} protein exhibited constitutively high levels of tyrosine phosphorylation indistinguishable from the parental

gp185^{erbB-2} protein (Fig. 3A). Conversely, both the EGFR/*erbB-2*^{COOH} chimeric protein and the parental EGFR showed a low basal level of tyrosine phosphorylation, which was markedly increased upon EGF stimulation. These results indicated that the two chimeric receptor proteins were enzymatically active and intrinsically capable of coupling with intracellular mitogenic signaling pathways.

The 32D-EGFR/*erbB-2*^{COOH} cells proliferated specifically in response to EGF stimulation (Fig. 3B). In contrast, 32D-*erbB-2*/EGFR^{COOH} cells were indistinguishable from control 32D in their inability to form colonies in the absence of added IL-3 (Fig. 3B). These findings argued that the COOH-terminal domains of EGFR and *erbB-2* were not responsible for the observed specificity of

their mitogenic signaling in 32D cells and strongly suggested that this specificity must be determined by the tyrosine kinase domain. This conclusion was supported by analysis of chimeras between *v-erbB* and Δ *NerbB-2* (20). The LTR-*v-erbB/erbB-2*^{COOH} expression vector, which encoded a protein containing the *v-erbB* tyrosine kinase domain and the COOH-terminal domain of *erbB-2*, conferred IL-3 independence to 32D cells (Fig. 3B). In contrast, the Δ *NerbB-2/v-erbB*^{COOH} expression vector, which contained the tyrosine kinase domain of *erbB-2* and the COOH-terminal domain of *v-erbB*, did not do so (Fig. 3B).

As a final test, we constructed chimeras in which the tyrosine kinase domains of EGFR and *erbB-2* were reciprocally switched. These chimeras, designated EGFR/*erbB-2*^{TK} and *erbB-2/EGFR*^{TK} (21), were transfected into 32D and NIH 3T3 cells. The 32D-EGFR/*erbB-2*^{TK} exhibited about 1/10 the colony formation of 32D-EGFR (Fig. 4). Conversely, the specific transforming activity of the EGFR/*erbB-2*^{TK} chimera for NIH 3T3 cells was approximately 100 times higher than that of the parental EGFR construct (Fig. 4).

The 32D cells expressing the *erbB-2/EGFR*^{TK} chimera formed colonies at high efficiency in the absence of IL-3, whereas 32D-*erbB-2* cells did not proliferate under the same conditions (Fig. 4). Yet, this chimera had an efficiency $\leq 1/100$ that of the parental *erbB-2* in inducing transformation of NIH 3T3 cells (Fig. 4). All of these results localized the domain responsible for the reciprocal differences in abilities of EGFR and *erbB-2* to couple with mitogenic pathways in 32D and NIH 3T3 cells to a 270-amino acid stretch encompassing their respective tyrosine kinase domains. The tissue- or cell-specific differences observed establish the distinct nature of EGFR and *erbB-2* intracellular signaling.

Although the tyrosine kinase domain was critical to the specificity of mitogenic signal transduction, we observed no significant role of the more divergent COOH-terminal domains. These findings argue that this domain may have regulatory importance, but is not critical for effective signal coupling. Analogously, the conserved tyrosine kinase domain of the insulin receptor has recently been reported to be important in signal transduction independent of its catalytic activity (22). The construction of additional chimeras should aid in further localization of the site or sites within the tyrosine kinase domain required for efficient EGFR function in 32D cells. At the same time, efforts to characterize recently identified receptor kinase substrates including the *raf* kinase (23), phospholipase C- γ (24), and GAP (25) may provide additional insights into the basis for specificity in mitogenic signaling by the EGFR and *erbB-2* products

in different target cells.

In many instances oncogene-mediated alterations appear to be tumor-specific. For example, the *erbB-2* gene is amplified and overexpressed in a significant fraction of mammary adenocarcinomas (10, 26). Conversely, EGFR amplification and overexpression has been frequently detected in squamous cell carcinomas and glioblastomas (11). In model systems, the targeting of expression of oncogenes in transgenic mice has also resulted in significant variations in tissue-specific sensitivity to tumor induction (27). Our present findings suggest that tissue-specific differences in the availability of intracellular components of mitogenic signaling pathways may account for the selection of specific oncogenes in certain tumors.

REFERENCES AND NOTES

- P. Kahn and T. Graf, Eds., *Oncogenes and Growth Control* (Springer-Verlag, New York, 1986); G. Guroff, *Oncogenes, Genes, and Growth Factor* (Wiley Interscience, New York, 1987).
- J. H. Pierce *et al.*, *Science* **239**, 628 (1988).
- M. F. Roussel *et al.*, *Nature* **325**, 549 (1987); E. Livneh *et al.*, *J. Biol. Chem.* **261**, 12490 (1986).
- A. O. Morla, J. Schreurs, A. Miyajima, J. Y. Wang, *Mol. Cell. Biol.* **8**, 2214 (1988); D. H. Madoff, T. M. Martensen, M. D. Lane, *Biochem. J.* **15**, 252 (1988); A. Sengupta *et al.*, *Proc. Natl. Acad. Sci. U.S.A.* **85**, 8062 (1988); R. Isfort, R. D. Huhn, A. R. Frackelton, J. N. Ihle, *J. Biol. Chem.* **263**, 19203 (1988).
- P. P. Di Fiore *et al.*, *Science* **237**, 178 (1987).
- P. P. Di Fiore *et al.*, *Cell* **51**, 1063 (1987).
- J. N. Ihle, L. Peppersack, L. Rebar, *J. Immunol.* **126**, 2184 (1981); J. N. Ihle, J. Keller, L. Henderson, F. Klein, E. W. Palascynski, *ibid.* **129**, 2431 (1982); M. B. Prystowsky *et al.*, *ibid.*, p. 2337; J. S. Greenberger *et al.*, *Proc. Natl. Acad. Sci. U.S.A.* **80**, 2931 (1983).
- Stable transfected 32D cell lines were isolated according to a modification of a method of electroporation [F. Toneguzzo *et al.*, *Mol. Cell. Biol.* **6**, 703 (1986)] as previously described (2).
- R. C. Mulligan and P. Berg, *Proc. Natl. Acad. Sci. U.S.A.* **78**, 2072 (1981).
- J. Yokota *et al.*, *Lancet* **i**, 765 (1986); M. H. Kraus, N. C. Popescu, S. C. Amsbaugh, C. R. King, *EMBO J.* **6**, 605 (1987); M. van de Vijver, R. van de Berselaar, P. Devilee, C. Cornelisse, J. Peterse, R. Nusse, *Mol. Cell Biol.* **7**, 2019 (1987); H. Lacroix, J. D. Iglehart, M. A. Skinner, M. H. Kraus, *Oncogene* **4**, 145 (1989).
- G. T. Merlino *et al.*, *Science* **224**, 417 (1984); Y. H. Xu, N. Richert, S. Ito, G. T. Merlino, I. Pastan, *Proc. Natl. Acad. Sci. U.S.A.* **81**, 7308 (1984); C. R. King *et al.*, *Nucleic Acids Res.* **13**, 8477 (1985).
- O. Segatto, C. R. King, J. H. Pierce, P. P. Di Fiore, S. A. Aaronson, *Mol. Cell. Biol.* **8**, 5570 (1988).
- G. Carpenter and S. Cohen, *Annu. Rev. Biochem.* **48**, 193 (1979); J. Schlessinger, *J. Cell Biol.* **103**, 2067 (1986); W. S. Chen *et al.*, *Nature* **328**, 820 (1987); A. M. Honnegger *et al.*, *Cell* **51**, 199 (1987); W. H. Moolenaar *et al.*, *EMBO J.* **7**, 707 (1988).
- The expression vector LTR- Δ *NACerbB-2* was engineered by modifying the previously described LTR-1- Δ *NerbB-2* plasmid (5). The latter plasmid contained unique engineered Eco RI and Mlu I sites in the 3' untranslated region after the natural *erbB-2* stop codon. To obtain the COOH-terminal truncation in LTR- Δ *NACerbB-2*, LTR-1- Δ *NerbB-2* was depleted of the coding sequence encompassed between the Sca I site at position 3737 of the *erbB-2* sequence (18) and the mentioned Eco RI site. The Eco RI site was rendered blunt-ended and self-ligation of the plasmid was performed. The joining of the Sca I end to the blunt-ended Eco RI end
- created an in-frame TAA stop codon. The translation of the NH₂- and COOH-truncated *erbB-2* protein begins at a methionine 32 amino acids proximal to the transmembrane region (5) and terminates at glutamic acid at position 1195 of the original *erbB-2* sequence (18). This construction, and all of the other constructions described in this study, were sequenced in the junction regions to verify that the predicted structure was achieved after the recombination procedures.
- B. Vennstrom, L. Fanshier, C. Moscovici, J. M. Bishop, *J. Virol.* **36**, 575 (1980); T. Yamamoto *et al.*, *Cell* **35**, 71 (1983).
- The LTR-*v-erbB* expression vector was engineered starting from the LTR-2 vector previously described (5) and the AEV-11 plasmid containing the genome of the ES4 isolate of the avian erythroblastosis virus (15). A 2.1-kb Pst I-Eco RI fragment of AEV-11, encompassing the *v-erbB* open reading frame, was cloned in the LTR-2 vector digested with Pst I and Bam HI. Joining between the Eco RI and the Bam HI sites at the 3' of the coding sequence was obtained with an oligonucleotide of the following structure AATTCCCACAGCACAGCTGTGGACAACCCCTGAGTATCTTGTAGTGAACGCGTG-ATC. This oligonucleotide contained information to restore the last 14 amino acids of the *v-erbB* sequence (ES4 isolate), an in-frame stop codon and a unique Mlu I site.
- P. P. Di Fiore *et al.*, unpublished observation.
- L. Coussens *et al.*, *Science* **230**, 1132 (1985); A. Ullich *et al.*, *Nature* **309**, 418 (1984).
- The LTR-EGFR/*erbB-2*^{COOH} and LTR-*erbB-2/EGFR*^{COOH} expression vectors were engineered starting from the LTR-EGFR (6) and LTR-*erbB-2* (5) plasmids. A conserved Bcl I site, at position 3009 and 3021 of the original *erbB-2* and EGFR sequence, respectively (18) and a unique Cla I site, contained in the M-MuLV sequence after the stop codons of both genes in the LTR vectors, were used for the recombination. Both LTR-EGFR and LTR-*erbB-2* were digested with Bcl I and Cla I. A 2.1-kb Bcl I-Cla I fragment from LTR-*erbB-2*, containing the 3' of *erbB-2* cDNA, was ligated to the 11.2-kb Bcl I-Cla I fragment of the LTR-EGFR containing the EGFR cDNA depleted of its 3' terminus, to yield the LTR-EGFR/*erbB-2*^{COOH} expression vector. The reciprocal recombination yielded the LTR-*erbB-2/EGFR*^{COOH} expression vector; in the latter case, because of the presence of a second Bcl I site at position 3078 in the EGFR cDNA (18), an oligonucleotide was used to restore the 19 codons of EGFR encompassed between the two Bcl I sites.
- Expression vectors LTR-*v-erbB/erbB-2*^{COOH} and Δ *NerbB-2/v-erbB*^{COOH} were obtained starting from the *v-erbB* (16) and Δ *NerbB-2* (5) plasmids. It is to be noted that the tyrosine kinase domain of *v-erbB* is virtually identical to the analogous sequence in the chicken EGFR [I. Lax *et al.*, *Mol. Cell. Biol.* **8**, 1970 (1988)] and shows only one nonconservative amino acid change with respect to the human sequence (18). The switch of the COOH-terminal domains was obtained taking advantage of the unique Bcl I (18, 19) site located at the border between the tyrosine kinase and COOH domains and the unique Mlu I site (5, 14, 16) located after the stop codon in the above-mentioned constructions. The strategy employed was similar to that described for the engineering of the LTR-EGFR/*erbB-2*^{COOH} and LTR-*erbB/EGFR*^{COOH} expression vectors (19).
- The LTR-EGFR/*erbB-2*^{TK} and LTR-*erbB-2/EGFR*^{TK} expression vectors were engineered starting from the LTR-EGFR (6) and LTR-*erbB-2* (5) plasmids. A novel Sal I site was engineered, in homologous positions, in the sequences of EGFR and *erbB-2* immediately after the transmembrane region, by site-directed mutagenesis according to Kunkel [T. A. Kunkel, *Proc. Natl. Acad. Sci. U.S.A.* **82**, 488 (1985)] (see also Fig. 4). The Sal I sites were engineered modifying the sequence GGAGGC [nucleotides (nt) 2225-2230] and GGAGAC (nt 2213-2218) of the EGFR and *erbB-2* open reading frames, respectively, to GTCGAC. These modifications did not alter the predicted protein sequences of EGFR and *erbB-2*. The newly engineered Sal I site and the conserved Bcl I site, previously described (19), were used for the recombination. An 0.8-kb Sal I-Bcl I fragment from LTR-*erbB-2*, containing

- the tyrosine kinase region of *erbB-2*, was ligated to the 12.3 Sal I-Bcl I fragment of the LTR-EGFR containing the EGFR cDNA depleted of its tyrosine kinase region, to yield the LTR-EGFR/*erbB-2*^{TK} expression vector. The reciprocal recombination yielded the LTR-*erbB-2*/EGFR^{TK} expression vector; in the latter case, because of the presence of a second Bcl I site at position 3078 in the EGFR cDNA (18), an oligonucleotide was used to restore the 19 codons of EGFR encompassed between the two Bcl I sites.
22. M. F. White *et al.*, *Cell* **54**, 641 (1988).
 23. D. K. Morrison, D. R. Kaplan, U. Rapp, T. M. Roberts, *Proc. Natl. Acad. Sci. U.S.A.* **85**, 8855 (1988); D. K. Morrison *et al.*, *Cell* **58**, 649 (1989).
 24. M. I. Wahl *et al.*, *Mol. Cell. Biol.* **9**, 2934 (1989); J. Meisenhelder, P. G. Suh, S. G. Rhee, T. Hunter, *Cell* **57**, 1109 (1989); B. Margolis *et al.*, *ibid.*, p. 1101.
 25. C. J. Molloy *et al.*, *Nature* **342**, 711 (1989).
 26. D. J. Slamon *et al.*, *Science* **235**, 177 (1987).
 27. C. J. Quaipe, C. A. Pinkert, D. M. Ornitz, R. D. Palminter, R. L. Brinster, *Cell* **48**, 1023 (1987); Y. Suda *et al.*, *EMBO J.* **6**, 4055 (1987); W. J. Muller, E. Sinn, P. K. Pattengale, R. Wallace, P. Leder, *Cell* **54**, 105 (1988).
 28. Antisera were prepared against synthetic peptides derived from the predicted amino acid sequences of EGFR and *erbB-2* (18). Antipeptide antibodies M1, M6, and M7 were obtained by immunizing rabbits

with synthetic peptides derived from the *erbB-2* sequence (18), encompassing residues 866–880, 1218–1232, and 1240–1255, respectively (18). The antibodies E5 and E7 were obtained against synthetic peptides derived from the EGFR predicted sequence (18), encompassing residues 985–990 and 1172–1186, respectively (18). The αF antipeptide antibody, directed against the protein kinase C modulation domain of the EGFR, was a kind gift of J. Schlessinger.

29. We thank D. Bottaro and C. Molloy for making available the antiphosphotyrosine antibody and C. Kinicley for providing technical assistance.

10 August 1989; accepted 12 February 1990

The Effect of Electrical Coupling on the Frequency of Model Neuronal Oscillators

THOMAS B. KEPLER, EVE MARDER, L. F. ABBOTT

Neurons with oscillatory properties are a common feature of the nervous system, but little is known about how neural oscillators shape the behavior of neuronal networks or how network interactions influence the properties of neural oscillators. Mathematical models are used to examine the effect of electrically coupling an oscillatory neuron to a second neuron that is either silent or tonically firing. Models of oscillatory neurons with varying degrees of complexity show that this coupling can either increase or decrease the frequency of an oscillator, depending on its membrane potential wave form, the state of the neuron to which it is coupled, and the strength of the coupling. Thus, electrical coupling provides a flexible mechanism for modifying the behavior of an oscillatory neural network.

NEURONS THAT DISPLAY INTRINSIC oscillatory properties are important components of many biological neural networks (1, 2). In particular, networks that generate rhythmic motor patterns often use neurons with oscillatory membrane properties (2). Despite considerable advances in our understanding of rhythmic neural networks, we do not know precisely how the frequency of such networks is controlled. Recent studies of the pyloric network of the lobster stomatogastric ganglion (STG) showed that the frequency of the oscillator anterior burster (AB) neuron is influenced by electrical coupling to other neurons (3). Specifically, in the presence of the peptide proctolin the frequency of the pacemaker-driven network was about 1 Hz, whereas the frequency of the isolated AB neuron was about 2 Hz; in this study the investigators concluded that the electrically coupled neurons were providing a “load” on the pacemaker, slowing it down (3).

We are currently developing network models that contain oscillatory elements (4).

While studying the effect of electrical coupling on an oscillating neuron within these models, we found that the situation is not nearly as simple as the “loading” picture would imply. Instead, electrical coupling provides a flexible way of modulating the frequency of an oscillator that depends critically on properties of the oscillator and of the coupled cell and on the coupling strength.

We begin by considering the effect of electrical coupling in a simple model of a bursting neuron based on a modified form of the FitzHugh-Nagumo equations (5). In this approach we do not model individual action potential spikes but consider a cell membrane potential v with action potentials either removed or averaged over. In the particular case of the STG, this is a good approximation because its neurons release neurotransmitter as a graded function of membrane potential, and action potentials contribute little (6). In the general case, it is reasonable because the integrated contribution of a given action potential spike to the current through the resistive coupling is quite small.

To construct the model, we divide the total current entering or leaving the cell into four parts, the capacitive current $C dv/dt$, an external current I , a fast component of the membrane current $f(v)$, and a slow mem-

brane current s . By current conservation,

$$C \frac{dv}{dt} = -f(v) - s + I \quad (1)$$

The slow component of the membrane current is determined by another differential equation

$$\tau \frac{ds}{dt} = \alpha v - s \quad (2)$$

The parameter τ determines the time scale for variations of s . In contrast to the usual approach (5), our fast current $f(v)$ is purely resistive but at intermediate membrane potentials it has a negative-resistance region that connects two positive-resistance regions at low and high potentials.

Depending on the exact form of $f(v)$ and on the values of the parameters C , α , and τ , neurons modeled by these equations can be oscillatory, can display plateau properties, can be tonically active, or can be silent. For the oscillatory case, the neuron can be predominantly hyperpolarized (top left of Fig. 1) or predominantly depolarized (top right of Fig. 1) during its cycle, depending on the value of an additive constant in the expression for $f(v)$.

To explore the effects of electrical coupling, we take for the “external” current

$$I = g(v_p - v) \quad (3)$$

where g determines the strength of the electrical coupling and v_p is the membrane potential of a passive cell to which the oscillator is coupled. The membrane current for the passive cell is modeled as purely resistive and fast, so including the electrical coupling to the oscillator we have

$$C_p \frac{dv_p}{dt} = -G_p(v_p - \bar{v}_p) + g(v - v_p) \quad (4)$$

Here \bar{v}_p is the resting potential and G_p is the conductance of the passive cell in the absence of electrical coupling.

Figure 1 shows the result of increasing the coupling conductance between a hyperpolarized passive cell and two different oscillators. It is clear that the effect of electrical

T. B. Kepler and E. Marder, Department of Biology and Center for Complex Systems, Brandeis University, Waltham, MA 02254.

L. F. Abbott, Department of Physics and Center for Complex Systems, Brandeis University, Waltham, MA 02254.